Article ID: 1000-5773(2010)02-0113-07

Structural Stabilities and Optical Properties of BaX (X=S, Se and Te) under High Pressure*

HAO Ai-Min[1], YANG Xiao-Cui[2], ZHAO Yu-Wei[1], LIU Xin[1],
SONG Ai-Jun[1], ZHANG Wei-Guo[1], XIN Wei[1]

(1. *College of Physics and Chemistry, Hebei Normal University of Science and Technology, Qinhuangdao* 066004, *China*;
2. *Department of Physics, Baicheng Normal University, Baicheng* 137000, *China*)

Abstract: An investigation on the structural stabilities and optical properties of BaX (X=S, Se and Te) under high pressure was conducted using first-principles calculations based on density functional theory. The results show that the sequence of the pressure-induced phase transition of these compounds is from the NaCl-type (B1) to the CsCl-type (B2) structure. The structural transition pressure and the metallization pressure are 8.57 and 45.4 GPa for BaS, 7.44 and 36.5 GPa for BaSe, 5.67 and 16.7 GPa for BaTe, respectively. The calculation of the optical properties showed that almost all peaks of the imaginary part of dielectric constant (ε_2) in the B1 and B2 structures shift towards high-energy region with increasing pressure (blue shift), and the static dielectric constant increases as the pressure increases.

Key words: first-principles; structural transition; optical property; high pressure; dielectric constant

CLC number: O521.2 **Document code**: A

1 Introduction

The alkaline-earth chalcogenides (AX: A=Mg, Ca, Sr, Ba; X=O, S, Se, Te) form a very important closed shell ionic system crystallizing in the NaCl-type (B1) structure at normal conditions except MgTe. These compounds are technologically valuable materials with many applications from catalysis to microelectronics[1]. Moreover, they have also been applied in the area of luminescent devices[2].

The pressure-induced structural transition of the alkaline-earth chalcogenides has been studied extensively[3-12]. These compounds undergo a transition from the B1 ($Fm3m$) to the B2 ($Pm3m$) structure under high pressure. For example, barium chalcogenides are found to exhibit the structural transition at 6.5, 6.0 and 4.8 GPa, respectively[3-5]. Apart from this, these compounds demonstrate an interesting phenomenon of metallization under compression[6-7].

Metallization is often described in terms of the single-particle band states as the overlap of the filled valence band and the unoccupied conduction band[8]. The band gaps in these closed-shell materials are expected to decrease as the pressure increases, until finally the empty d-type conduction band drops in energy below the top of the filled p-type valence bands. Ba chalcogenides are particularly

* **Received date**: 2009-04-10; **Revised date**: 2009-08-17
Foundation Item: China Postdoctoral Science Foundation (20090450924), Doctoral Foundation of Hebei Normal University of Science and Technology (2008YB001)
Author Biography: HAO Ai-Min(1964—), male, Ph. D., professor, major in high-pressure physics.
E-mail: aiminhao1991@yahoo.com.cn

promising compounds for metallization since they have smaller band gaps and bulk moduli than those of other alkaline-earth chalcogenides.

Grzybowski *et al*. reported that the metallization of BaTe occurs at 20 GPa by resistivity measurement[5]. Ruoff *et al*. predicted that BaSe undergoes metallization at about 40 GPa on the basis of optical-absorption and resistivity measurement[6]. High-pressure optical-absorption data indicated that the metallization pressure of BaS is about 80 GPa[7].

In this paper, we present a comparative and complementary study of the electronic and optical properties to the previous experimental and theoretical works.

2 Computational Details

Our first-principles calculations were performed based on the plane wave basis set, the ultrasoft pseudopotential for the electron-ion interaction, and the exchange-correlation potential of Perdew *et al*. in the generalized gradient approximation (GGA) for electron-electron interaction[13]. The typical configuration is $5s^2 5p^6 6s^2$ for Ba, $3s^2 3p^4$ for S, $4s^2 4p^4$ for Se, and $5s^2 5p^4$ for Te. Integrations in the Brillouin zone (BZ) were performed using special k points generated with $14\times14\times14$ for the B1 and B2 structures. One-electron valence states were expanded on a basis of plane waves with a cutoff energy of 700 eV. Such parameters had been tested to be sufficient for convergence. During the structure optimizations, the total energy is minimized by varying lattice constants and internal atomic positions under the restriction of the given symmetry, and all forces on atoms were converged to be less 0.1 eV/nm. All the stress components were less than 0.02 GPa, the tolerance in the self-consistent field (SCF) calculation was 5.0 μeV/atom by using the finite basis set corrections[14].

3 Results and Discussions

3.1 Structural Properties

The total energy as a function of volume is calculated to determine the equilibrium volume and bulk modulus by parabolic fitting to a third-order Birch-Murnaghan equation of state[15]. Calculated equilibrium lattice constant (a_0) and bulk modulus (K) of BaS, BaSe, and BaTe in the B1 and B2 structures are illustrated in Table 1. It can be clearly seen that the calculated structural parameters are in excellent agreement with experimental results. The slight overestimation of the theoretical lattice constants is typical of GGA.

Table 1 Calculated equilibrium lattice constant and bulk modulii of the B1 and B2 structures of the three compounds at zero pressure

Material	Structure	Lattice constant a/(nm)		Bulk modulii K/(GPa)		
		Expt.	Theor.	Expt.	Theor. (Ref.)	Theor.
BaS	B1	0.634 7[19]	0.640 4	55.1±1.4[19]	52.5[18]	47.9
	B2		0.383 5	21.4±0.3[19]	60.8[18]	51.7
BaSe	B1	0.659 3[4]	0.661 9	43.4±2.6[6]	45.4[18]	41.0
	B2	0.379 5[4]	0.391 8	41.9±1.4[6]	52.9[18]	52.6
BaTe	B1	0.700 5[5]	0.701 7	29.4[6]	33.8[18]	34.4
	B2		0.421 2	27.5[6]	39.4[18]	41.3

Our computational approach is based on constant-pressure static quantum mechanical calculations at $T=0$ K, so the relative stability of different phases can be deduced from the pressure dependence of the enthalpy instead of the Gibbs free energy[16-19]. As shown in Fig. 1, the calculation suggests that

there exists a phase transition from the B1 to B2 phase that agrees with the experimental results. The pressure corresponding to $\Delta H = H - H_{B1}$ approaching zero is the phase transition pressure. At a pressure higher than the theoretical transition pressure, the B1 phase becomes thermodynamically unstable while the B2 phase becomes mechanically and thermodynamically stable. Our results are tabulated in Table 2, together with the available experimental data and the previous theoretical results for comparison. For the volume collapse, our results are in excellent agreement with the experimental and theoretical results. For the transition pressures, however, are overall higher than the experimental results. This is probably due to the fact that the experiments were carried out at room temperature, whereas the calculations assume $T=0$ K.

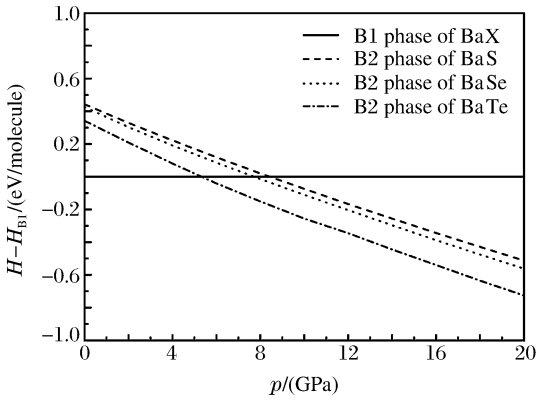


Fig. 1　Calculated enthalpies for the B2 phase of BaX (X=S, Se and Te) relative to that of the B1 phase as a function of pressure

Table 2　Transition pressures and volume collapses for the B1 to B2 transition pressures and metallization transition pressures of BaS, BaSe and BaTe

Material	Pressure	$\Delta V/V$/(%)			p_t/(GPa)		
		Expt.	Theor. (Ref.)	Theor.	Expt.	Theor. (Ref.)	Theor.
BaS	B1 to B2	13.7[3]	13.8[14]	13.3	6.5[3]	6.03[14]	8.57
	Metallization		0[14]	0	80.0[8]	49.1[14]	45.4
BaSe	B1 to B2	13.9[4]	13.4[14]	12.4	6.0[4]	5.20[14]	7.44
	Metallization		0[14]	0	52.0[8]	31.0[14]	36.5
BaTe	B1 to B2	13.2[5]	10.7[14]	12.0	4.8[5]	3.95[14]	5.67
	Metallization		0[14]	0	20.0[5]	14.1[14]	16.7

Among the three compounds, the metallization pressure of BaTe is lowest as a result of its smaller bulk modulus and band gap. From the analysis of the obtained transition and the metallization pressures, we can conclude that the transition pressure and the metallization pressure decrease with the atomic number of the cation or anion for isostructural compounds.

3.2　Band Structure

The self-consistent band structures of all three compounds have been obtained at ambient and high pressures, as shown in Fig. 2, where only BaS is illustrated since the overall band profile is found to be similar for all three compounds. Our results are in agreement with earlier works[20]. In the case of B1 structure, the gap is always indirect between the top of the chalcogen valence p band occurring at the Γ point and the bottom of the Ba $5d$ bands occurring at X. The shape of this conduction band is similar to that of the fcc noble or transition metals which is due to the fact the Ba atoms constitute a fcc sublattice. It can also be seen that the structural transition induces a large reduction in the band gap. Just after the structural transition, the band gaps are still indirect, except that now the valence p band of the chalcogen atom occurs at M and the bottom of Ba $5d$ conduction bands at Γ.

The gaps are still positive after the structural transition, indicating that the metallization occurs only after structural transition. For BaS and BaSe, the indirect gap transforms to a direct one at Γ before metallization. For BaTe, however, the indirect gap remains until band overlap occurs. Our result is

very well in agreement with the other theoretical work[18]. At metallization the band gap closes due to the overlap of the Ba 5*d* conduction bands and the chalcogen valence *p* bands which arise due to the broadening of the bands with increasing pressure.

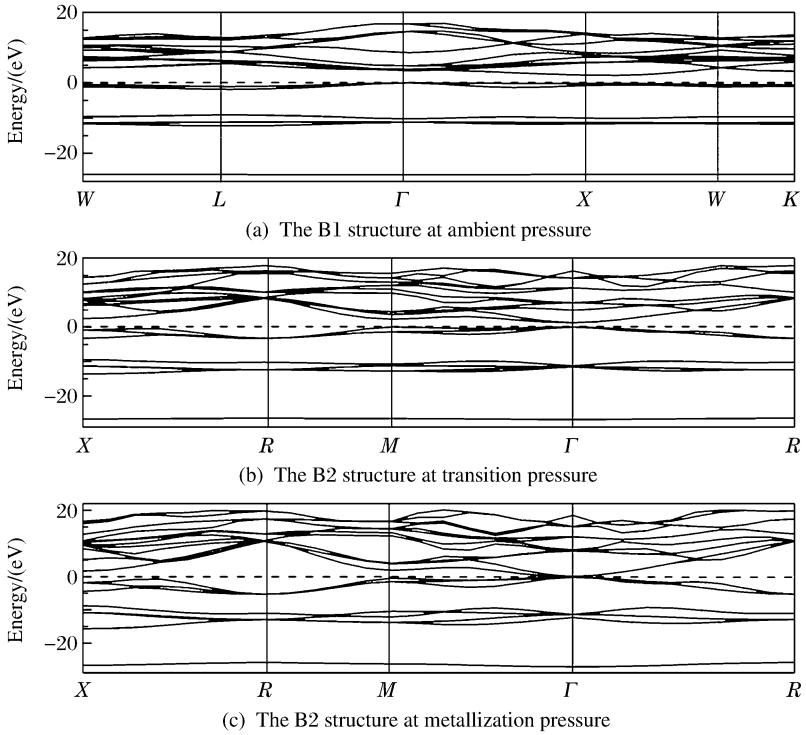


Fig. 2 The band structures of BaS

The pressure dependence of the band gaps in the B1 and B2 structures is shown in Fig. 3. The band gaps of the three compounds decrease monotonically with pressure. The calculated linear and quadratic pressure coefficients for the important band gaps are listed in Table 3. The linear pressure coefficients increase with the chalcogen atomic number. The underlying physical reasons for such a trend are likely produced by the coupled role of the larger pressure shift for the more delocalized *p* states of the heavier chalcogenides and the smaller bulk moduli associated with increasing ionic radii.

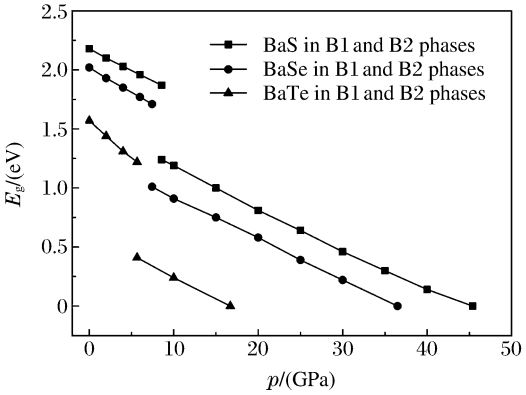


Fig. 3 The band gap as a function of pressure in the B1 and B2 structures of the three compounds

Table 3 The linear and quadratic coefficients of the important band gap in B2 phase

($E(p) = E_0 + bp + cp^2$, $b = \partial E/\partial p$ **in** 10^{-2} eV · GPa^{-1}, $c = \partial^2 E/2\partial^2 p$ **in** 10^{-4} eV · GPa^{-2})

Material	*M*-*M*		*M*-*Γ*		*Γ*-*Γ*	
	b	*c*	*b*	*c*	*b*	*c*
BaS	0.41	−0.11	−3.20	1.88	−4.43	1.85
BaSe	−0.33	0.37	−3.95	2.67	−5.10	2.72
BaTe	−2.45	2.95	−6.62	8.87	−7.14	8.38

The calculated value of band gap E_g in the B1 structure and the energy reduction ΔE at transition pressure are list in Table 4, along with the experimental value and the other theoretical works. The metallization pressures for the three compounds are given in Table 2. As can be seen from Table 2, the metallization pressures in our calculation are lower than the experimental results. The possible reason for the pressure deviation is ascribed to the following factors.

(1) The indication of metallization in experiments is the leveling off of the resistivity; while the metallization is characterized by the overlap of the energy band in the calculation. The different means lead inevitable to the difference between the experimental and theoretical results.

(2) The calculated band gaps at ambient conditions underestimate the measured ones by about 40%～50%. This discrepancy is due to the errors introduced by the GGA to the exchange-correlation potential and the neglect of the relativistic effect (spin-orbit interaction terms) in our calculations.

Table 4　The value of E_g and ΔE_v(B1) of the B1 structure at ambient pressure, together with ΔE and ΔE_v(B2) at the B1－B2 transition pressure　(eV)

Material	E_g[20]	E_g[18]	E_g	ΔE	ΔE_v(B1)	ΔE_v(B2)
BaS	3.9	2.3	2.17	0.64	1.9	3.3
BaSe	3.6	2.01	2.01	0.72	2.0	3.5
BaTe	3.4	1.58	1.67	0.82	2.2	3.9

The upper valence-band width ΔE_v is in part a measurement of the strength of the crystal field at the anionic sites, determined by the cation-anion distance, also depends on anion-anion overlap, i. e., second-nearest-neighbor interactions[21]. Our calculated results are listed in Table 4. Two conclusions can be derived: (1) the strength of the crystal field at the anionic site increases with the increasing atomic number of anion in an isoelectronic series; (2) the strength of the crystal field in the high pressure phase is larger than that in the ambient pressure phase for each of the three compounds.

3.3　Optical Properties

The optical properties of the B1 and B2 structures of the three compounds are also calculated. Denser k points (24×24×24) are sampled in the BZ, and the norm-conserving pseudopotential is used for accuracy[22]. Dielectric function $\varepsilon(\omega)$, which describes the features of linear response of the system to an electromagnetic radiation, governs the propagation behavior of radiation in a medium. $\varepsilon(\omega)$ is connected with the interaction of photons with electrons. Its imaginary part $\varepsilon_2(\omega)$ can be given by calculating the momentum matrix elements between the occupied and unoccupied wave functions within the selection rules, and its real part $\varepsilon_1(\omega)$ can be derived from $\varepsilon_2(\omega)$ by the Kramer-Kronig relations. All the other optical parameters, such as refractive index $n(\omega)$, absorption coefficient $\alpha(\omega)$, reflectivity $R(\omega)$ and electron energy-loss spectrum $L(\omega)$ can be deduced from $\varepsilon_1(\omega)$ and $\varepsilon_2(\omega)$[23]. Here, we discuss the case of incident radiation with the linear polarization along the [100] direction. The calculated $\varepsilon_2(\omega)$ of BaS in the B1 and B2 structures is shown in Fig. 4. From the graph, we found that almost all peaks of ε_2 in the B1 and B2 structures shift towards high-energy region with increasing pressure (blue shift). An abnormal shift (red shift) of the second peak in the B2 structure is observed under high pressure.

The static dielectric constant $\varepsilon(0)$, one of the important optical parameters, is also calculated under high pressures. The pressure dependence of $\varepsilon(0)$ is illustrated in Fig. 5. As can be seen from Fig. 5, the static dielectric constants increase with pressure. This is because, as the applied pressure increases, the atomic distance becomes shorter, which results in a increase of photons reflected by media. In addition, a sudden increment of the static dielectric constants is observed as the B1 phase

transforms into the B2 phase. This is because the density of electronic state suddenly increases during the phase transition.

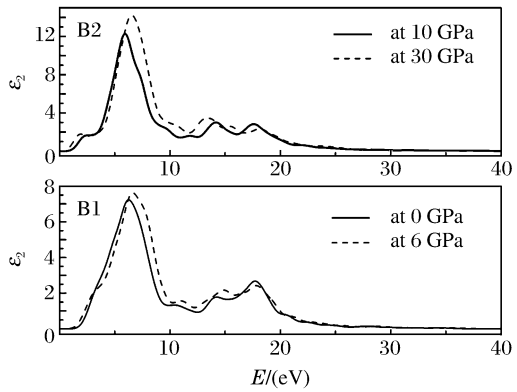


Fig. 4 The calculated $\varepsilon_2(\omega)$ of BaS in the B1 and B2 structures under high pressures

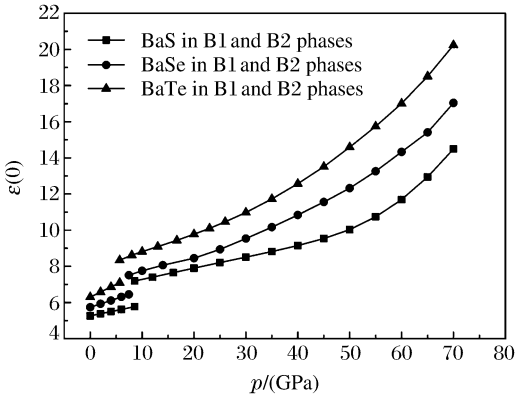


Fig. 5 The static dielectric constants $\varepsilon(0)$ as a function of pressure of the B1 and B2 structures for the three compounds

4 Conclusions

The structural stabilities and optical properties of BaX (X=S, Se and Te) under high pressure have been investigated using first-principles calculations based on density functional theory. The results demonstrate that the sequence of the pressure-induced phase transitions of the three compounds is from the B1 to B2 structure, moreover the structural transition pressures and metallization pressures are 8.57 and 45.4 GPa for BaS, 7.44 and 36.5 GPa for BaSe, and 5.67 and 16.7 GPa for BaTe. The calculation of the optical properties showed that, as the pressure increases, the static dielectric constant augments, and almost all peaks of the imaginary part of dielectric constant (ε_2) in the B1 and B2 structures shift towards high-energy region (blue shift), except the second peak in the B2 structure.

References:

[1] Khenata R, Baltache H, Rérat M, et al. First-Principle Study of Structural, Electronic and Elastic Properties of SrS, SrSe and SrTe under Pressure [J]. Physica B: Condens Matter, 2003, 339(4): 208-215.

[2] Pandey R, Sivaraman S. Spectroscopic Properties of Defects in Alkaline-Earth Sulfides [J]. J Phys Chem Solids, 1991, 52(1): 211-225.

[3] Yamaoka S, Shinomura O, Nakazawa H, et al. Pressure-Induced Phase Transformation in BaS [J]. Solid State Commun, 1980, 33(1): 87-89.

[4] Grzybowski T A, Ruoff A L. High-Pressure Phase Transition in BaSe [J]. Phys Rev B, 1983, 27(10): 6502-6503.

[5] Grzybowski T A, Ruoff A L. Band-Overlap Metallization of BaTe [J]. Phys Rev Lett, 1984, 53(5): 489-492.

[6] Minomura S. Solid State Physics under Pressure [M]. 1st ed. Tokyo: Terra Scientific Press, 1985: 57-61.

[7] Weir S T, Vohra Y K, Ruoff A L. Pressure-Induced Metallization of BaSe [J]. Phys Rev B, 1987, 35(2): 874-876.

[8] Ross M, McMahan A K. Systematics of the $s \rightarrow d$ and $p \rightarrow d$ Electronic Transition at High Pressure for the Elements I through La [J]. Phys Rev B, 1982, 26(8): 4088-4093.

[9] Pourghazi A, Dadsetani M. Electronic and Optical Properties of BaTe, BaSe and BaS from First Principles [J]. Physica B: Condens Matter, 2005, 370(1-4): 35-45.

[10] Bouhemadou A, Khenata R, Zegrar F, et al. *Ab Initio* Study of Structural, Electronic, Elastic and High Pressure Properties of Barium Chalcogenides [J]. Comput Mater Sci, 2006, 38(2): 263-270.

[11] Charifi Z, Baaziz H, Hassan F E H, et al. High Pressure Study of Structural and Electronic Properties of Calcium

Chalcogenides [J]. J Phys Condens Matter,2005,17(26):4083-4092.
[12] Tuncel E,Colakoglu K,Deligoz E,et al. A First-Principles Study on the Structural,Elastic,Vibrational,and Thermodynamical Properties of BaX (X=S,Se,and Te) [J]. J Phys Chem Solids,2009,70(2):371-378.
[13] Perdew J P,Burke K,Ernzerhof M. Generalized Gradient Approximation Made Simple [J]. Phys Rev Lett,1996,77(18):3865-3868.
[14] Francis G P,Payne M C. Finite Basis Set Corrections to Total Energy Pseudopotential Calculations [J]. J Phys Condens Matter,1990,2(19):4395-4404.
[15] Birch F. Finite Strain Isotherm and Velocities for Single-Crystal and Polycrystalline NaCl at High-Pressures and 300 Degrees K [J]. J Geophys Res,1978,83(4):1257-1268.
[16] Ma Y,Eremets M,Oganov A R,et al. Transparent Dense Sodium [J]. Nature,2009,458(7235):182-185.
[17] Ma Y,Oganov A R,Li Z,et al. Novel High Pressure Structures of Polymeric Nitrogen [J]. Phys Rev Lett,2009,102(6):065501.
[18] Kalpana G,Palanivel B,Rajagopalan M. Electronic Structure and Structural Phase Stability in BaS,BaSe,and BaTe [J]. Phys Rev B,1994,50(17):12318-12325.
[19] Weir S T,Vohra Y K,Ruoff A L. High-Pressure Phase Transitions and the Equations of State of BaS and BaO [J]. Phys Rev B,1986,33(6):4221-4226.
[20] Kaneko Y,Morimoto K,Koda T. Optical Properties of Alkaline-Earth Chalcogenides. II. Vacuum Ultraviolet Reflection Spectra in the Synchrotron Radiation Region of 4～40 eV [J]. J Phys Soc Jpn,1983,52(12):4385-4396.
[21] Zimmer H G,Winzen H,Syassen K. High-Pressure Phase Transitions in CaTe and SrTe [J]. Phys Rev B,1985,32(6):4066-4070.
[22] Hamann D R,Schlüter M,Chiang C. Norm-Conserving Pseudopotentials [J]. Phys Rev Lett,1979,43(20):1494-1497.
[23] Saha S,Sinha T P. Electronic Structure,Chemical Bonding,and Optical Properties of Paraelectric $BaTiO_3$ [J]. Phys Rev B,2000,62(13):8828-8834.

高压下钡的硫化物的结构相变和光学性质研究

郝爱民[1],杨晓翠[2],赵玉伟[1],刘　鑫[1],宋爱君[1],张卫国[1],辛　伟[1]

(1.河北科技师范学院理化学院,河北秦皇岛　066004;
2.白城师范学院物理系,吉林白城　137000)

摘要:利用基于密度泛函的第一性原理,计算了高压下钡的硫化物(BaS、BaSe 和 BaTe)的结构相变和光学性质。计算结果表明,这些化合物的压致结构相变是从 NaCl 型结构转变为 CsCl 型结构;对于结构转变压力和金属化转变压力,BaS 为 8.57 GPa 和 45.4 GPa,BaSe 为 7.44 GPa和 36.5 GPa,BaTe 则分别为 5.67 GPa 和 16.7 GPa。光学性质计算结果显示:随着压力的增加,静态介电常数 ε_0 不断增加,介电常数虚部 ε_2 的峰值向高能方向移动(蓝移)。

关键词:第一性原理;结构转变;光学性质;高压;介电常数

中图分类号:O521.2　　**文献标识码**:A